MODELLING AND CONTROL OF AN ALUMINIUM STRIP UNWINDER-REWINDER

Sylvain Leirens[1], **Joseph Pierquin**

Pechiney - Centre de Recherches de Voreppe
725, rue Aristide Bergès BP 27 - 38341 Voreppe Cedex - France
joseph.pierquin@pechiney.com

Keywords: Aluminium strip processing, modelling, tension control, decoupling control.

Abstract

In an aluminium strip processing line, the main concern is to control independently velocity and tension. This paper deals with two control systems applied to a basic unwinder-rewinder system: the first one is based on classic PI controllers including specific compensations. The second is a LQG control. Simulations demonstrate the effectiveness of both solutions.

1 Introduction

Modern high-speed process lines demand good tension control for maximum efficiency [1][2]. In an aluminium strip processing line, tension control is required in many operations (rolling, coating, washing...). For such systems, it is very important to prevent the occurrence of strip break by decoupling the strip tension and the strip velocity [1]. The strong coupling between both variables is induced by the strip elasticity: a physical modelling of this process is given in section 2. Generally, on industrial production lines, the control is based on simple PID techniques and the know-how of the operators [3]: it is often non-optimal with low dynamic performances. The first control strategy presented in this paper is an optimised PI control including specific disturbance compensations: it is based on the inversion principle of the physical modelling deduced from the general laws of physics (c.f. section 3). The second is a LQG control based on an optimal statistical Kalman filtering (c.f. section 4). Both strategies are compared and show an ability to decouple velocity and tension.

2 System Modelling

A continuous aluminium strip processing line typically can be described as a system of rolls and a strip stretched between them [4]. This is the simplest unit of a continuous strip process. At each side, a motor provides torque to the roll. Our laboratory prototype exhibits the inherent problems of metal transport system (see figure 1). An induction motor (3 kW) drives the rewinder: it provides torque to the roll with high dynamic through a rotor field oriented control. A pneumatic brake is used for the unwinder. Two load cells measure the tension in the aluminium strip. An incremental encoder implemented on a non-motorized roll measures the linear speed. Both acquisition and control systems are implemented in real time on a Matlab-Simulink/dSpace^{TM} 1103 card software-hardware package.

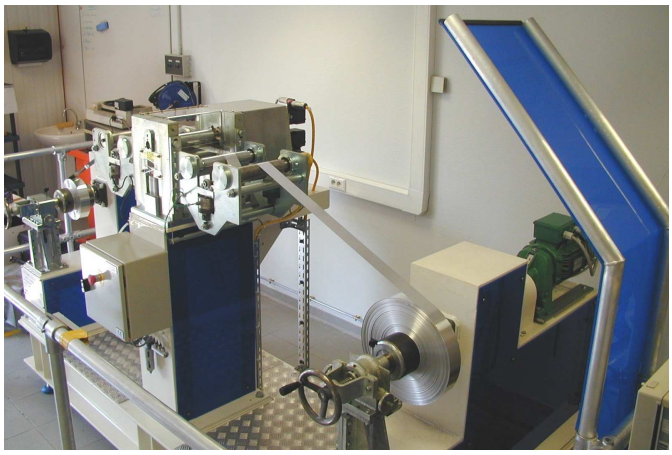

Figure 1: Laboratory prototype

A simplified diagram is given in figure 2. The gear ratio between motor and roll is one to one. It is assumed that there is no slip between roll and strip.

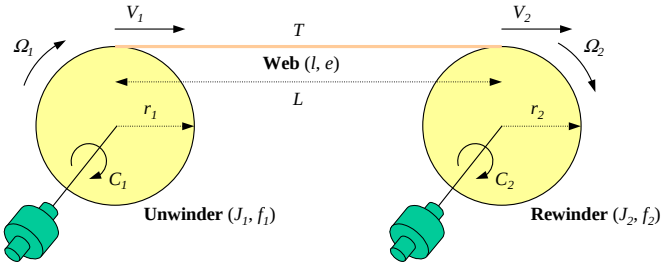

Figure 2: Unwinding-Rewinding system

The aim of this study is to build a model of this system. First, a mathematical model of both rolls and strip tension dynamics is established. Second, this model is developed under a state-model form.

[1]That work has been performed to meet requirements of Sylvain Leirens's end of studies internship with Pechiney. Sylvain Leirens is now with the ASH Team of Supelec (sylvain.leirens@supelec.fr), Avenue de la Boulaie, BP 81127 35511 CESSON-SEVIGNE Cedex - France.

Nomenclature

L	:	Span length (m)
l	:	Span width (m)
e	:	Span thickness (m)
A	:	Cross-sectional area of web (mm^2)
ρ	:	Density of aluminium strip (kg/m^3)
E	:	Modulus of elasticity (Pa)
V_i	:	Strip velocity (m/s)
T	:	Strip tension force (N)
r_i	:	Roll radius (m)
r_0	:	Empty roll radius (m)
J_i	:	Polar moment of inertia of roller (kg.m^2)
J_{i0}	:	Polar moment of inertia of empty roller (kg.m^2)
f_i	:	Friction coefficient (kg.m^2/s.rad)
Ω_i	:	Roll rotational speed (tr/mn)
C_i	:	Torque (N.m)

2.1 Strip tension force

The system under consideration is the *piece of strip between the unwinder and the rewinder* whose length L is assumed to be constant. It is a typical *mass flow* system.
Moreover, the strip is assumed not to be strained beyond its limit of elasticity.
The mass balance equation is:

$$\left(\frac{\mathrm{d}}{\mathrm{d}t}\begin{bmatrix}\textit{mass stored}\\ \textit{in the system}\end{bmatrix}\right) = \begin{pmatrix}\textit{input}\\ \textit{mass flow}\end{pmatrix} - \begin{pmatrix}\textit{output}\\ \textit{mass flow}\end{pmatrix}. \quad (1)$$

The strip density is assumed to be constant. Equation (1) gives:

$$\frac{\mathrm{d}}{\mathrm{d}t}\left[\int_0^L A(x,t)\,\mathrm{d}x\right] = A_1(t)V_1(t) - A_2(t)V_2(t) \quad (2)$$

where subscripts $_1$ and $_2$ denote unwinder and rewinder respectively.
Considering an infinitesimal element of span (length $\mathrm{d}x$), element stretching can be written as:

$$\mathrm{d}x = \big(1+\epsilon(x,t)\big)\mathrm{d}x_u. \quad (3)$$

Both unstretched (subscript $_u$) and stretched element volume are equal:

$$\mathrm{d}v = A(x,t)\,\mathrm{d}x = A_u(x,t)\,\mathrm{d}x_u. \quad (4)$$

A combination of (3) and (4) takes the following form:

$$A(x,t) = \frac{A_u(x,t)}{1+\epsilon(x,t)}. \quad (5)$$

Equation (2) gives:

$$\frac{\mathrm{d}}{\mathrm{d}t}\left[\int_0^L \frac{A_u(x,t)}{1+\epsilon(x,t)}\,\mathrm{d}x\right] = A_{1u}(t)V_1(t) - \frac{A_{2u}(t)}{1+\epsilon_2(t)}V_2(t) \quad (6)$$

considering that the tension force in the strip of the unwinder roll is neglected in comparison with T.
When the span is not stretched, $A_u = A_{1u} = A_{2u}$ and (6) can be simplified:

$$\frac{\mathrm{d}}{\mathrm{d}t}\left[\int_0^L \frac{1}{1+\epsilon(x,t)}\,\mathrm{d}x\right] = V_1(t) - \frac{V_2(t)}{1+\epsilon_2(t)}. \quad (7)$$

Assuming that $\epsilon \ll 1$, high order terms can be neglected: $1/(1+\epsilon) \approx 1-\epsilon$. Equation (7) becomes:

$$\frac{\mathrm{d}}{\mathrm{d}t}\left[\int_0^L \big(1-\epsilon(x,t)\big)\,\mathrm{d}x\right] = V_1(t) - V_2(t)\big(1-\epsilon_2(t)\big). \quad (8)$$

Meanwhile supposing that the strain ϵ does not vary with x, *i.e.* $\epsilon(x,t) \approx \epsilon_2(t)$, (8) can be written as:

$$-L\frac{\mathrm{d}\epsilon_2}{\mathrm{d}t} = V_1(t) - V_2(t)\big(1-\epsilon_2(t)\big), \quad (9)$$

so:

$$L\frac{\mathrm{d}\epsilon_2}{\mathrm{d}t} = V_2 - V_1 - \epsilon_2 V_2 \quad (10)$$

omitting time t.
Using Hooke's law, *i.e.* $\epsilon_2 = T/AE$ and notation $\frac{\mathrm{d}}{\mathrm{d}t}(\ ) = \dot{(\ )}$, equation (10) gives:

$$L\dot{T} = AE(V_2 - V_1) - TV_2. \quad (11)$$

Considering small variations around a steady-state operating point:

$$\begin{aligned} V_1 &= V_{10} + \Delta V_1,\\ V_2 &= V_{20} + \Delta V_2,\\ T &= T_0 + \Delta T. \end{aligned}$$

Then we have:

$$L\frac{\mathrm{d}\Delta T}{\mathrm{d}t} + V_{20}\Delta T = AE(\Delta V_2 - \Delta V_1). \quad (12)$$

With s the Laplace variable, (12) becomes:

$$(Ls + V_{20})\Delta T = AE(\Delta V_2 - \Delta V_1), \quad (13)$$

which gives:

$$\Delta T = \frac{AE}{Ls + V_{20}}(\Delta V_2 - \Delta V_1). \quad (14)$$

Omitting the notation "Δ" to improve readability, Equation (14) can be written as a classic first order transfer:

$$T = \frac{K_b}{T_b s + 1}(V_2 - V_1) \quad (15)$$

where $K_b = AE/V_{20}$ et $T_b = L/V_{20}$.

2.2 Roll dynamics

Details are given for the unwinder (which is similar to the winder). Radii vary with time and their expressions take the following form by writing roll surfaces S_i [5]:

$$S_1(t) = \pi\, r_1^2(t), \tag{16}$$

then differentiating with respect to time:

$$\dot{S}_1 = 2\pi\, r_1\, \dot{r}_1 \tag{17}$$

omitting time t.
And

$$\dot{S}_1 = -V_1\, e = -r_1\, \Omega_1\, e. \tag{18}$$

Hence:

$$\Omega_1\, e = -2\pi\, \dot{r}_1, \tag{19}$$

so:

$$\dot{r}_1 = -\frac{\Omega_1\, e}{2\pi}. \tag{20}$$

As radius r_1, inertia J_1 is time-varying too:

$$(J_1\dot{\Omega}_1) = \dot{J}_1\Omega_1 + J_1\dot{\Omega}_1 \tag{21}$$

with:

$$J_1 = J_{1motor} + J_{1roll} \tag{22}$$

so:

$$J_1 = J_{10} + \underbrace{\frac{1}{2}\pi\rho\, l\, r_1^4 - \frac{1}{2}\pi\rho\, l\, r_0^4}_{wound\ strip}. \tag{23}$$

J_1 can be written as:

$$J_1 = J_{1constant} + J_{1variable} \tag{24}$$

which is the sum of a constant inertia $J_{1constant}$ and a variable inertia $J_{1variable}$. Hence:

$$J_{1constant} = J_{10} - \frac{1}{2}\pi\rho\, l\, r_0^4, \tag{25}$$

$$J_{1variable} = \frac{1}{2}\pi\rho\, l\, r_1^4. \tag{26}$$

Differentiating (26) with respect to time:

$$\dot{J}_1 = 2\pi\rho\, l\, \dot{r}_1 r_1^3. \tag{27}$$

The dynamic principle applied to a rotation movement gives:

$$(J_1\dot{\Omega}_1) = C_{1d} - C_{1c} \tag{28}$$

where C_{1d} et C_{1c} denote driving and load torques respectively:

$$C_{1d} = C_1 + Tr_1, \tag{29}$$

$$C_{1c} = f_1\Omega_1. \tag{30}$$

It gives:

$$(J_1\dot{\Omega}_1) = C_1 + Tr_1 - f_1\Omega_1. \tag{31}$$

Similarly, we obtain for the rewinder:

$$\begin{array}{l} \dot{r}_2 = \frac{\Omega_2\, e}{2\pi}, \\ \dot{J}_2 = 2\pi\rho\, l\, \dot{r}_2 r_2^3, \\ (J_2\dot{\Omega}_2) = C_2 - Tr_2 - f_2\Omega_2. \end{array} \tag{32}$$

2.3 Models

Nonlinear time-varying model

Using results above, the model below was built:

$$\left\{\begin{array}{l} \dot{J}_1\Omega_1 + J_1\dot{\Omega}_1 = Tr_1 + C_1 - f_1\Omega_1 \\ \dot{J}_2\Omega_2 + J_2\dot{\Omega}_2 = C_2 - Tr_2 - f_2\Omega_2 \\ J_1 = a_1 + b_1 r_1^4 \\ J_2 = a_2 + b_2 r_2^4 \\ \dot{J}_1 = 2\pi\rho\, l\, \dot{r}_1 r_1^3 \\ \dot{J}_2 = 2\pi\rho\, l\, \dot{r}_2 r_2^3 \\ \dot{r}_1 = -\frac{\Omega_1\, e}{2\pi} \\ \dot{r}_2 = \frac{\Omega_2\, e}{2\pi} \\ V_1 = r_1\Omega_1 \\ V_2 = r_2\Omega_2 \\ L\dot{T} = AE(V_2 - V_1) - TV_2 \end{array}\right. \tag{33}$$

where :

$$\left\{\begin{array}{l} a_i = J_{i0} - \frac{1}{2}\pi\rho\, l\, r_0^4 \\ b_i = \frac{1}{2}\pi\rho\, l \end{array}\right.$$

with $i = 1, 2$.
This model requires knowledge of J_{10}, J_{20}, r_0, r_{10} et r_{20}.

Linear time-invariant model

Assuming that inertiae change slowly compared to the strip dynamics, therefore radii and inertiae are considered as constant now. In addition, we detail the model by considering torque loops of our asynchronous motors. Calling C_i^* the torque reference, a first order system is used to represent this loop :

$$\frac{C_i}{C_i^*} = \frac{1}{T_c s + 1} \tag{34}$$

where $i = 1, 2$ and T_c is the time constant of the torque loop.

As before, the results above are collected and the following model is (see figure 3):

$$\left\{\begin{array}{l} \Omega_1 = \frac{1}{J_1 s + f_1}(C_1 + Tr_1) \\ \Omega_2 = \frac{1}{J_2 s + f_2}(C_2 - Tr_2) \\ C_1 = \frac{1}{T_c s + 1} C_1^* \\ C_2 = \frac{1}{T_c s + 1} C_2^* \\ V_1 = r_1\Omega_1 \\ V_2 = r_2\Omega_2 \\ T = \frac{K_b}{1 + T_b s}(V_2 - V_1) \end{array}\right. \tag{35}$$

where :

$$\left\{\begin{array}{l} J_i = a_i + b_i r_i^4 \\ a_i = J_{i0} - \frac{1}{2}\pi\rho\, l\, r_0^4 \\ b_i = \frac{1}{2}\pi\rho\, l \end{array}\right. .$$

with $i = 1, 2$.
This model requires knowledge of V_{10}, J_{10}, J_{20}, r_0, r_1 et r_2.

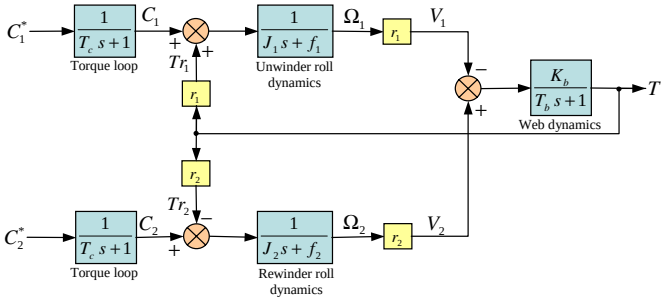

Figure 3: Linear time-invariant model

Figure 3 shows the strong coupling between the speed V_2 and the strip tension T. Whenever speed changes, it affects tension trough the difference $\Delta V = V_1 - V_2$. Variations of tension disturb the speed through the load torque Tr_2 as well.

Finally, the state-form of the linear time-invariant model can be written.
With vectors:

$$X = \begin{pmatrix} C_1 \\ C_2 \\ \Omega_1 \\ \Omega_2 \\ T \end{pmatrix}, \quad U = \begin{pmatrix} C_1^* \\ C_2^* \end{pmatrix} \; and \quad Y = \begin{pmatrix} T \\ V_2 \end{pmatrix},$$

and matrix:

$$\mathcal{A} = \begin{pmatrix} -\frac{1}{T_c} & 0 & 0 & 0 & 0 \\ 0 & -\frac{1}{T_c} & 0 & 0 & 0 \\ \frac{1}{J_1} & 0 & -\frac{f_1}{J_1} & 0 & \frac{r_1}{J_1} \\ 0 & \frac{1}{J_2} & 0 & -\frac{f_2}{J_2} & -\frac{r_2}{J_2} \\ 0 & 0 & -\frac{K_b r_1}{T_b} & \frac{K_b r_2}{T_b} & -\frac{1}{T_b} \end{pmatrix},$$

$$\mathcal{B} = \begin{pmatrix} \frac{1}{T_c} & 0 \\ 0 & \frac{1}{T_c} \\ 0 & 0 \\ 0 & 0 \\ 0 & 0 \end{pmatrix} \; and \quad \mathcal{C} = \begin{pmatrix} 0 & 0 & 0 & 0 & 1 \\ 0 & 0 & 0 & r_2 & 0 \end{pmatrix},$$

the state-model is obtained:

$$\begin{cases} \dot{X} = \mathcal{A}X + \mathcal{B}U \\ Y = \mathcal{C}X \end{cases}. \tag{36}$$

3 PI-based control

An optimised PI-based control is proposed here. PID control techniques are often considered as non-adapted to control velocity and tension independently [3]. In fact industrial control schemes are non-optimised. The proposed strategy is based on the model inversion principle [6]. Modelling of physical phenomena has allowed a good understanding of the way the energy is converted in the system. Therefore, the system can be efficiently controlled by appropriate corrections and compensations [6].

3.1 Control design

To control the strip linear velocity V_2, we choose to work on the motor of the rewinder (see figure 4). This choice is classic [1]. The strong problem comes from the coupling between V_2 and T through Tr_2. The influence of Tr_2 must be compensated in the tension control loop (see figure 4). Then a PI-controller (called Speed PI-2) is tuned (c.f. section 3.2). Its tuning is based on mechanical and torque loop dynamics (modelled as first order transfers). Using this type of controller, the static error (step response) is cancelled.

In the same way, to control the strip tension T, we choose to work on V_1 through C_1. Therefore we use a similar structure to the rewinder speed loop and tune two PI-controllers (called Speed PI-1 and Tension-PI). The first one is calculated by using mechanical and torque loop dynamics (similar to V_2 speed loop). The second one is based on strip and V_1 speed loop dynamics. The controller output $\Delta V^* = V_2^* - V_1^*$ (* denotes reference) allows to obtain V_1^* using the reference V_2^*.

This control is based on the compensation of load torques Tr_1 and Tr_2. These torques disturb loops significantly and the quality of compensation is very important. We use the strip tension model to improve the dynamic of these compensations (see figure 4). Furthermore, it is necessary to use reference V_2^* to obtain efficient feedforward action on the tension controller output.

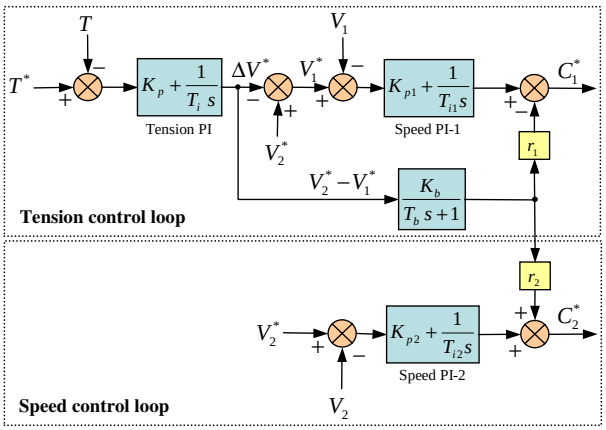

Figure 4: PI-based control scheme

3.2 PI controllers tuning

The model of the system is rewritten as follows:

$$H_{bo}(s) = \frac{K}{(T_1 s + 1)(T_2 s + 1)} \tag{37}$$

where T_1 et T_2 denote the small (parasitic) and large time constants respectively.
PI controllers have the following form:

$$C_{PI}(s) = \frac{K_p(T_i s + 1)}{T_i s} \tag{38}$$

where K_p et T_i denote proportional gain and integral constant (s) respectively.

The tuning of controllers must be effective to obtain good decoupling between tension force and velocity. The compensated open loop transfer function is given by:

$$HC_{bo}(s) = \frac{K_p(T_i s + 1)}{T_i s} \frac{K}{(T_1 s + 1)(T_2 s + 1)} \tag{39}$$

and corresponding Bode diagram is represented on figure 5.

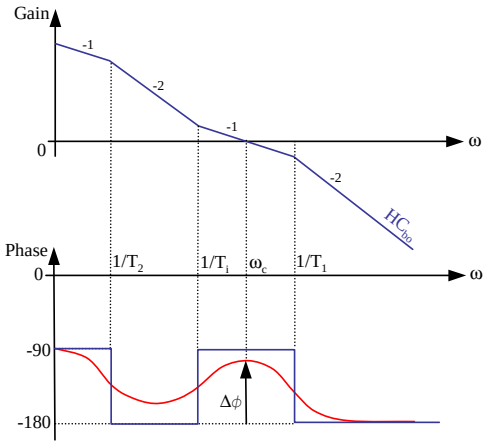

Figure 5: Compensated open loop Bode diagram

To reach a compromise between fast response and disturbance reject, the crossover pulsation is placed in the middle of the segment $[1/T_i, 1/T_1]$ which has a -1 slope [7]. The time constant T_i is calculated as follows:

$$\sin(\Delta\phi) = \frac{T_i - T_1}{T_i + T_1}. \tag{40}$$

For a phase margin $\Delta\phi$ equal to 37° which means an overshoot approximately equal to 30%, we obtain $T_i = 4T_1$. Then the crossover pulsation is equal to:

$$\omega_c = \frac{1}{\sqrt{T_i T_1}} = \frac{1}{2T_1}. \tag{41}$$

At this pulsation, we make the following approximation:

$$\frac{K K_p}{T_2 s} = 1 \tag{42}$$

which means:

$$K_p = \frac{T_2}{2KT_1}. \tag{43}$$

Theoretically, the relation $T_i/T_1 = 4$ can be considered as an optimum (*c.f.* Kessler's symmetrical optimum [7]). But in practice, this tuning is too fast and oscillations may appear. Therefore we can choose a factor greater than 4 ; the system will react more slowly. We can add a reference filter to compensate the zero induced by the PI controller too and decrease the overshooting. Such a filter has been implemented (not showed on the figure for better readability).

3.3 Simulation results

Results for step responses, 100 N for the tension and 1 m/s for the velocity are given figure 6.

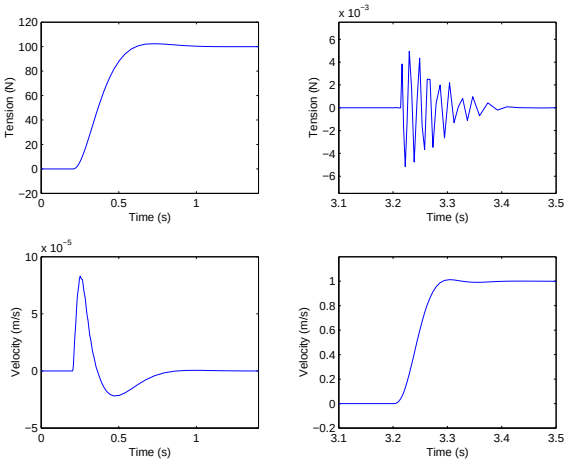

Figure 6: PI-based control

Figure 6 shows that the decoupling between tension and velocity is efficient. Interactions can be neglected compared to nominal values of velocity and tension.
Typical strategies are not able to decouple these variables with such a performance. It is important to note that this result could be achieved with standard PLC but requires accurate controllers tuning as well as the computation of compensations. This level of performance is easily obtained with advanced control strategies (see next section) but their implementation on standard material is more difficult.

4 State feedback control

In this part, a state approach is studied to build the controller. For this purpose, we use the state model (36) established in section 2.

4.1 Control design

For this purpose, a LQG control has been developed with an optimal statistical Kalman filtering to estimate the state of the system. The problem is formulated in standard form and the regulator is optimised using models of the process and its environment: the state model is enlarged taking into account predictive models of references and disturbances (see figure 7).

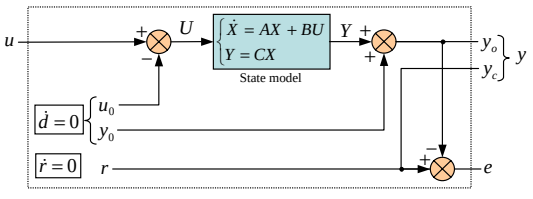

Figure 7: Deterministic standard model

These predictive models introduce an uncontrollable state part. The rejection of these modes allows to cancel the static error (presence of integrators).
To reach the compromise between performance and robustness, two high level synthesis parameters are used. The choice of weighting matrix is based on calculating partial grammians according to [8]: the tuning needs to specify two horizons, T_o and T_c for observation and control respectively.
Writing the gap $e = \mathcal{C}_e X$ between outputs and references, the controller has to minimize the criterium:

$$J = \int_0^\infty (e^T \mathcal{S}_c e + u^T \mathcal{R}_c u) \mathrm{d}t \tag{44}$$

where $\mathcal{S}_c$ and $\mathcal{R}_c$ have been chosen as follows:

$$\mathcal{S}_c = \mathcal{I}, \mathcal{R}_c = T_c \int_0^{T_c} (\mathcal{C}_e e^{\mathcal{A}t} \mathcal{B})^T (\mathcal{C}_e e^{\mathcal{A}t} \mathcal{B}) \mathrm{d}t. \tag{45}$$

To calculate the Kalman filter, we use noise variance matrix $\mathcal{S}_o$ and $\mathcal{R}_o$ as follows:

$$\mathcal{S}_o = \left[T_o \int_0^{T_o} e^{\mathcal{A}^T t} \mathcal{C}^T \mathcal{C} e^{\mathcal{A}t} \mathrm{d}t \right]^{-1}, \mathcal{R}_o = \mathcal{I}. \tag{46}$$

The horizon T_o tunes mainly the response time for the disturbance reject. The horizon T_c allows to manage the compromise between noise sensitivity of the control inputs and gain/phase margins.

4.2 Simulation results

Analysing the results for step responses, 100 N for the tension and 1 m/s for the velocity:

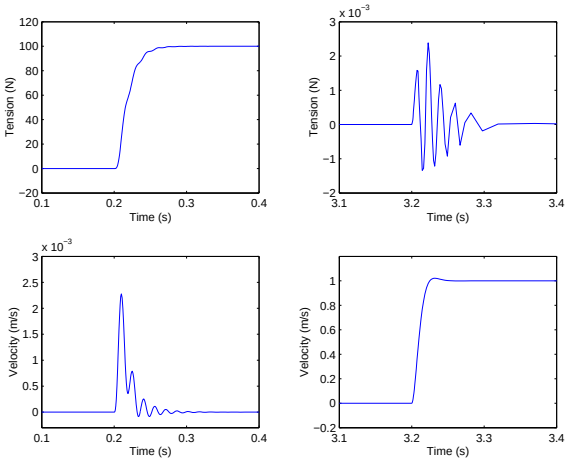

Figure 8: State feedback control

Figure 8 shows the decoupling between tension and velocity. The step responses are faster than those for the PI-based control.

5 Conclusion

For optimal control of an aluminium strip unwinder-rewinder, two control structures have been outlined. The first one is based on PI controllers : it is easily implementable on standard PLCs and gives good results. The second one uses a state approach and requires a powerful hardware/software system. The state feedback controller gives better results especially for the strip tension force. In both cases, the proposed controllers allow a good decoupling between strip tension and velocity.

References

[1] S. H. Jeon, J.-M. Kim, K.-C. Jung, S.-K. Sul, and J. Y. Choi. Decoupling control of bridle rolls for steel mill drive system. *IEEE Transactions on Industry Applications*, vol. 35, no1:pp. 119–125, January/Febraury 1999.

[2] D. Jouve and D. Bui. Digital servo drives for material tension control system. In *PCIM Conference*, Nuremberg (Germany), pp. 71-78, May 1996.

[3] H. Koç, O. Knittel, M de Mathelin, and G. Abba. Modelling and robust control of winding system for elastic webs. *IEEE Transaction on Control Systems Technology*, vol. 10, no2:pp. 197–208, March 2002.

[4] P. R. Pagilla. Robust observer-based control of an aluminium strip processing line. *IEEE Transactions on Industry Applications*, vol. 36, no3:pp. 865–870, May/June 2000.

[5] M. Humpich. *Contribution à l'étude d'une commande optimale multivariable en laminage monocage à froid des tôles minces*. PhD thesis, Ecole des mines de Paris, Université de Nice (France), 1988.

[6] S. Charlemagne, A. Bouscayrol, I. Slama-Belkhodja, and J.P. Hautier. Flatness based control of non-linear textile multimachine process. In *Proc. European Power Electronics Conference EPE 2003*, CD-ROM, Toulouse (France), September 2003.

[7] C. Kessler. Das symmetriche optimum. *Regelungstechnik*, vol. 6:pp. 432–436, 1958.

[8] P. de Larminat. *Contrôle d'état standard*. Collection pédagogique d'automatique. HERMES, 2000.